Nonappa, Nonappa; Haataja, Johannes S.; Timonen, Jaakko V.I.; Malola, Sami; Engelhardt, Peter; Houbenov, Nikolay; Lahtinen, Manu; Häkkinen, Hannu; Ikkala, Olli

Reversible Supracolloidal Self-Assembly of Cobalt Nanoparticles to Hollow Capsids and Their Superstructures

Published in:
Angewandte Chemie

DOI:
10.1002/anie.201701135

Published: 01/01/2017

Document Version
Peer-reviewed accepted author manuscript, also known as Final accepted manuscript or Post-print

COMMUNICATION

Reversible supracolloidal self-assembly of cobalt nanoparticles to hollow capsids and their superstructures

Nonappa[a]*, Johannes. S. Haataja[a], Jaakko. V. I. Timonen[a], Sami Malola[b], Peter Engelhardt[a,c], Nikolay Houbenov[a], Manu Lahtinen[d], Hannu Häkkinen[b]*, and Olli Ikkala[a]*

Abstract: There exists a growing need to master colloidal self-assembly towards ever more complex structures. Here we present a simple concept for synthesis and spontaneous, reversible supracolloidal hydrogen bond-driven self-assembly of cobalt nanoparticles (CoNPs) into hollow shell-like capsids and their directed assembly to higher order superstructures. CoNPs and capsids form in one step upon mixing dicobalt octacarbonyl (Co_2CO_8) and *p*-aminobenzoic acid (*p*ABA) in 1,2-dichlorobenzene using heating-up synthesis without additional catalysts or stabilizers. This leads to *p*ABA capped CoNPs (core ~5 nm) with a narrow size distribution. They spontaneously assemble into tunable spherical capsids (*d*~50-200 nm) with a few-layered shells, as driven by inter-nanoparticle hydrogen bonds via the carboxylic acid dimerization of the ligands. The capsids can be reversibly disassembled and reassembled by controlling the hydrogen bonds upon heating or solvent exchanges. The superparamagnetic nature of CoNPs allows magnetic field directed self-assembly of capsids to capsid chains. A sublety exists, as they remain stable even after removing the magnetic field due to an interplay of induced dipoles and inter-capsid hydrogen bonds. Finally, interfacial self-assembly by placing the capsids on water-air interface furnishes lightweight colloidal framework films. The presented spontaneous and reversible self-assembly of nanometer scale structural units (CoNPs) into shell-like units as driven by hydrogen bonds without amphiphilicity suggests the denotion as capsids. The synthetic colloidal capsids encourage towards new approaches and functions in encapsulation and confinement.

In material science, there is a growing need towards ever more advanced and hierarchical assemblies of colloids and nanoparticles.[1] Colloidal self-assembly is more difficult to master than the molecular self-assembly due to challenges in controlling the polydispersities, directionalities, and aggregations.[2] Still, several types of colloidal self-assemblies have been recently demonstrated using inorganic and organic structural units.[1-20] More specifically, related to colloidal self-assembly towards hollow structures, viral capsids provide inspiration via the hydrogen bond-driven reversible self-assembly of shape-matching proteinic units.[21] In synthetic chemistry, hollow spherical superstructures using colloids have been achieved using sacrificial templates, atomic layer deposition, and selective oxidation.[22] However, they typically involve templating, several steps, and purifications, and do not allow spontaneous and reversible disassembly and re-assembly of hollow capsid-like superstructures. Recently, water dispersible polydispersed CdS nanoparticles showed stabilizer-free spontaneous assembly into porous nanoshell-like structures.[23] The mechanism was attributed to electrostatic interactions, dispersion and other colloidal forces, supported by molecular dynamics simulations.

We recently reported template-free supracolloidal hydrogen bonded self-assembly of water-dispersible gold nanoclusters to 2D nanosheets and spherical capsids with monolayer thick shells by tuning the solvent conditions taken that the nanoclusters were atomically precise.[20] The self-assembly was driven by the ligands via carboxylic acid hydrogen bonding dimerization between the neighbouring nanoparticles. Such a self-assembly was attributed to the slightly non-spherical nature of the nanoparticles and the preferential alignment of hydrogen bonding ligands into the nanoparticle equatorial plane. However, the synthesis of atomically precise nanoclusters is laborious, and it becomes relevant to ask whether synthetic reversible capsids can be achieved by a simple and scalable synthesis.

Cobalt nanoparticles constitute a relevant model system to study nanoscale magnetic properties.[24a] A typical synthesis involves the hot-injection or heating-up method using dicobalt octacarbonyl $Co_2(CO)_8$ and surfactants (e.g. oleic acid or olely amine) in the presence of trioctyl phosphine oxide (TOPO).[24] The surfactants promote the dispersion and reduce aggregation in organic solvents, whereas TOPO catalyzes the decomposition of $Co_2(CO)_8$.

Here, we report a facile synthesis of superparamagnetic cobalt nanoparticles (CoNPs), their *in-situ* template-free reversible self-assembly to magnetic capsids driven by hydrogen bonds between the ligands, and their higher order superstructures by directed self-assembly. We envisaged ditopic ligands where one end selectively binds to CoNPs and simultaneously stabilizes them, whereas the other end makes hydrogen bonds between the CoNPs. Furthermore, we avoid additional catalysts/stabilizers as they might disturb the supramolecular interactions. We choose ditopic ligands containing amine ($-NH_2$) and carboxylic acid (-COOH) ends, as separated by a linker. Whereas the amine binds to the metal surface and stabilizes the nanoparticles, the carboxylic acid group allows inter-nanoparticle hydrogen bonding.

Our prototypical synthesis involves heating a mixture of $Co_2(CO)_8$ and *p*-aminobenzoic acid (*p*ABA) in 1.0/0.4 mol/mol ratio in 1,2-dichlorobenzene (1,2-DCB) from room temperature to 165 °C and holding at this temperature for 30 min (Figure 1a, see Supporting Information and Figure S1). The approach allows synthesis of CoNPs (*d*~5 nm) with *p*ABA ligands and their spontaneous *in situ,* template-free self-assembly to larger

[a] Prof. O. Ikkala, Dr. Nonappa, Prof. J. V. Timonen, M.Sc. J. S. Haataja
Department of Applied Physics, Aalto University School of Science
Puumiehenkuja 2, Espoo, FI-02150, Finland
E-mail: olli.ikkala@aalto.fi, nonappa@aalto.fi
[b] Prof. H. Häkkinen, Dr. S. Malola
Departments of Chemistry and Physics, Nanoscience centre
University of Jyväskylä, Survontie 9, FI-40014, Jyväskylä, Finland
E-mail: hannu.j.hakkinen@jyu.fi
[c] Dr. P. Engelhardt
Department of Pathology and Virology, Haartman Institute,
University of Helsinki, P.O. Box 21, FIN-00014, Helsinki, Finland
[d] Dr. M. Lahtinen
Department of Chemistry, University of Jyväskylä, Survontie 9, FI-40014, Jyväskylä, Finland
Supporting information for this article is given via a link at the end of the document.

spherical superstructures of sizes ~200 nm after cooling to room temperature (Figure 1b-e, cryo-TEM and dynamic light scattering in Figure S2). Electron tomographic reconstruction (ET) shows that the spherical superstructures possess ca. 25-30 nm thick shells of densely packed CoNPs (Figure 1f, Videos S1-S3), and there is no packing order within the shells (Figure S3). Such shell-like nanoparticle assemblies are here denoted as capsids, as will be discussed later. The individual nanoparticle sizes can be tuned from 5 nm to 10 nm by dcreasing the mole fraction of *p*ABA *vs.* $Co_2(CO)_8$ from 0.4 to 0.06. At the same time, the average capsid diameter is decreased from ca. 200 nm to 80 nm (Figure 1g and Figure S4). The contrast difference between the shells and interiors varies among the capsids (Figure 1b-d). However, 3D reconstructions revealed that the shell thickness of the capsids remains similar (~25 nm, Figure S3). The contrast difference is attributed to different levels of kinetically trapped *p*ABA ligands, which are not bound to cobalt. The capsids without trapped *p*ABA show a clear difference between the shell (dark) and interior (white) in their 2D projection (Figure 1c). On the otherhand, capsids with more trapped *p*ABAs show less contrast difference in their 2D projection (Figure 1d).

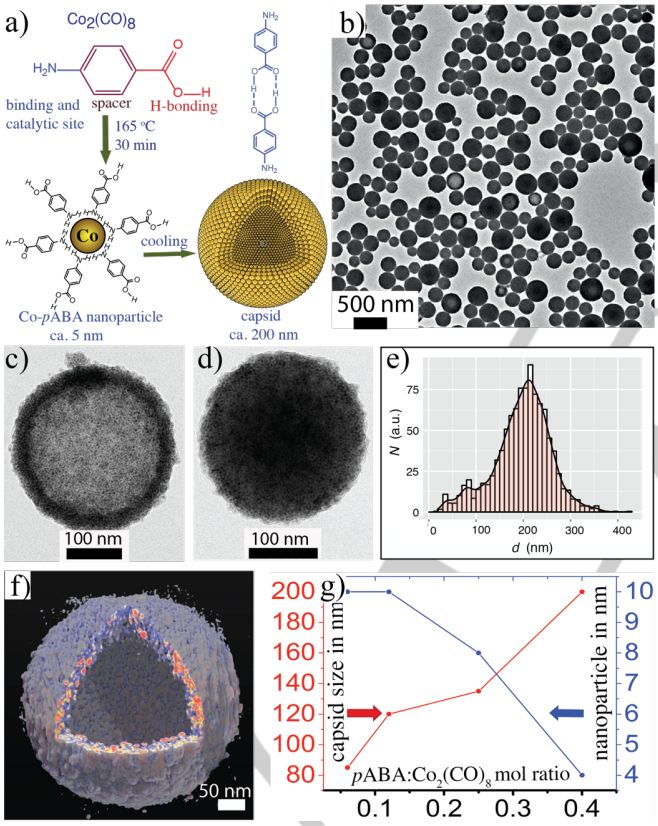

Figure 1. The overall concept. a) Cobalt nanoparticles by heating-up synthesis of $Co_2(CO)_8$ and *p*ABA in 1,2-DCB and their spontaneous self-assembly to shell-like capsids. b) TEM micrographs showing spherical capsids for $Co_2(CO)_8$/*p*ABA 1.0/0.4 mol/mol. Examples of capsids with less (c) and more (d) of kinetically trapped *p*ABA in the interior. e) Size distribution of capsids. f) Electron tomographic reconstruction resolves clearly the CoNP shell layer from the hollow interior (see Figure S3 for ET reconstruction of a capsid with trapped *p*ABA in the interior). g) The nanoparticle and capsid sizes are tunable by the composition.

The excess *p*ABA molecules can be removed by soaking the capsids in acetone (Figure 2a-c and Figure S5, S6), as *p*ABA is soluble in acetone, and the trapped *p*ABAs are transported through the porous shell in analogy to processes in colloidosomes,[25] as revealed by ET reconstruction (Figure 2c, Videos S4 & S5). That the capsid interior can contain trapped unbound *p*ABAs is also suggested by the ^1H and ^{13}C NMR spectroscopy (Figure S7) and can be controlled by processing kinetics (Figure S8).

We will next show that carboxylic acid hydrogen bonding between the ligands of the neighbouring Co-*p*ABA nanoparticles is important for the capsid formation. A direct evidence for existence of hydrogen bonds is obtained by FT-IR (Figure S9). Indirect evidence is provided by solvent and thermal induced reversibility. The capsids disassemble into individual nanoparticles (*d*~5 nm) in methanol (Figures 2d-e, and S10) due to the disruption of inter-nanoparticle hydrogen bonds. After dispersing the capsids in methanol, the excess *p*ABA molecules were removed by repeated washing and centrifugation. This allows colloidal dispersion without any unbound *p*ABA. When the purified CoNPs were redispersed in 1,2-DCB, they re-assembled into hollow spherical capsids (Figures 2f and S10), suggesting that the self-assembly is template-free. Further, when a solution of *p*ABA in 1,2-DCB was added to the purified dispersion of CoNPs, they reassembled into hollow capsids. However, the presence of *p*ABA resulted in capsid chains. Secondly, heating of Co-*p*ABA capsids in 1,2-DCB to ~150 °C resulted in disassembly to individual nanoparticles and reassembly upon cooling to room temperature (Figure 2g-h).

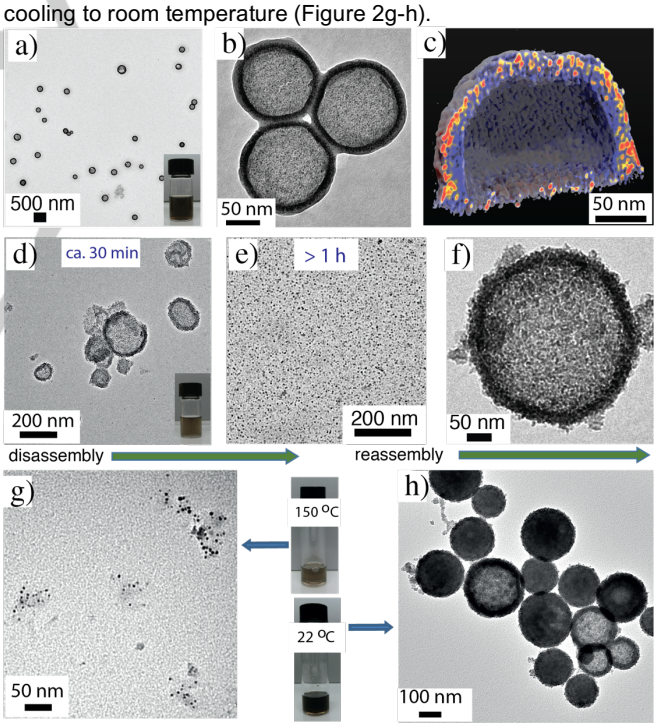

Figure 2. Thermal and solvent exchange driven reversibility of the capsids prepared from $Co_2(CO)_8$/*p*ABA 1.0/0.4 mol/mol. a) TEM micrographs of capsids after dispersing in acetone, the trapped *p*ABA ligands are removed. b) Interacting capsids in acetone as mediated by *p*ABA hydrogen bondings at the interfaces. c) h) ET reconstruction of an acetone treated capsid. TEM micrographs showing the disassembly of the capsids upon dispersing in methanol for d) 30 min and, e) > 1h. f) The capsids reassemble upon transferring to 1,2-DCB. The capsids dis-assemble upon heating (g) and reassemble upon cooling (h), i.e., show thermoreversibility.

This is expected as in pure benzoic acid the hydrogen bonding dimerization constant is reduced to ca. 4% from the room

temperature value upon heating to 150 °C in a medium with dielectric constant of 9.93, corresponding to 1,2-DCB (see Supporting Information for details and Figures S11, S12).[26]

Note that the reversible self-assembly of the CoNPs to spherical capsids with a few layered thick shell takes palce without any amphiphilicity of the building units, i.e. unlike vesicles, dendrosomes, and polymersomes whose molecular conformation is adjustable upon packing.[27] In our system we deal with the hydrogen bond driven packing of structurally rigid colloidal level building blocks (metal nanoparticles, Figure S3) to spherical superstructures. We denote these assemblies as capsids, as inspired by the viral capsids, that are formed by the H-bonding self-assembly of proteinic subunits.

To emphasize the novelty, we next describe ligands that do not allow capsids (see Figure 3a). First, random aggregates instead of capsids are obtained when heating-up synthesis was performed with only $Co_2(CO)_8$ suggesting the imporatnce of ligands. Similarly, no capsids were formed with a mixture of $Co_2(CO)_8$/TOPO, therein, the single functional group binds on metal core, and the peripheral moiety is nonfunctional. Importantly, heating up synthesis of a mixture of $Co_2(CO)_8$,TOPO and *p*ABA also furnished random aggregates(Figure S13), indicating that the presence of additional stabilizers interferes with nanoparticle formation and self-assembly. Unlike *p*ABA, the *ortho*- and *meta*- isomers, *o*ABA and *m*ABA did not lead to the capsids, where the steric hindrance of carboxylic groups limits the interparticle hydrogen bonding (Figure S14). Capsids were neither observed if the peripheral group of the ligand forms only weak hydrogen bonds, such as the hydroxyl-hydroxyl hydrogen bond between two aminophenols. These findings suggest that the key to capsid formation is in the ditopic structure of the ligands, containing a metal binding amino group and a hydrogen bonding peripheral carboxylic acid motif with a linker.

The role of hydrogen bonding in capsid formation, binding energy, diffusion barrier for ligand rearrangements, and magnetic moments of a model spherical cluster Co_{13}-*p*ABA_{12} was studied using density functional theory (DFT). We used spin-polarized density-functional theory with projector augmented waves (PAW) as implemented in the real-space grid code-package GPAW,[28] to study the ground state electronic structure and binding of *p*ABA ligands to model Co_{13} clusters (Figure 3b). The technical details on theoretical calculations are presented in the supporting information.

Optimized structures of the model clusters and molecules are shown in Figure 3b. Bare cobalt cluster Co_{13} and the core of the fully protected cluster Co_{13}*p*ABA_{12} are of the same symmetry. The average binding energy of one *p*ABA molecule in the Co_{13}*p*ABA_{12} cluster is 0.62 eV (Table S1). It is interesting to note that the calculated diffusion barrier for one *p*ABA molecule on top of the Co_{13} cluster is of the same order (~0.6 eV, see Figure 3c). This suggests facile ligand rearrangement around nanoparticle surface. The ligand-protected Co_{13} cluster has a relatively large magnetic moment of 1.6 Bohr magneton per atom.

We also looked at the interaction between the *p*ABA dimers and the modification of the interaction by methanol (Figure 3b, panels C,E). The *p*ABA dimer is bonded by 0.39 eV/hydrogen bond. The bonding becomes slightly weaker (0.35 eV/hydrogen bond) in the presence of methanol. This indicates the possibility that methanol disturbs the capsid formation, as also observed experimentally. Because of the curvature of the ligand surface, each Co_{13}*p*ABA_{12} cluster can make just a few hydrogen bonds to neighbouring clusters, leaving pores between the clusters (see Figure 3b, panel D).

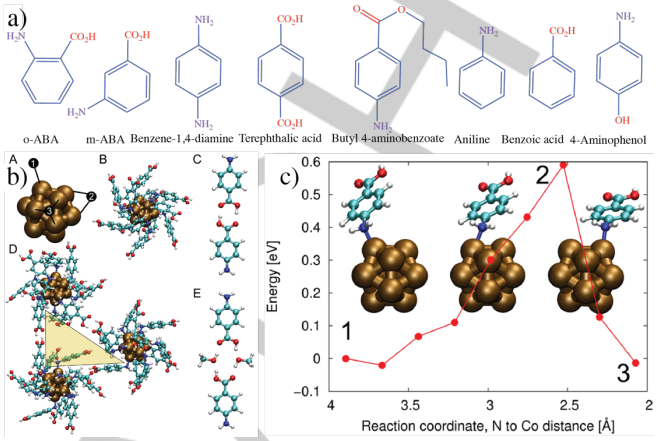

Figure 3. Understanding the ligands. a) Ligands that do not render capsids. b) Computational modelling: (A) Co_{13} model cluster; (B) Co_{13}*p*ABA_{12} model structure showing amines binding to nanoparticle surface leaving –COOH for inter-particle hydrogen bonding; (C) Hydrogen bonded *p*ABA dimer; (D) Trimeric superstructure showing a triangular pore due to packing frustration; (E) Hydrogen bonding in the *p*ABA-methanol complex. c) Diffusion barrier for a *p*ABA movement between two Co-top sites in the Co_{13}*p*ABA_{12} cluster. The diffusion barrier was calculated by using constrained relaxation. The reaction coordinate is defined as the distance between the N atom of *p*ABA and the Co atom where it is bound at configuration #3.

In order to explain in detail the thin shell formation, the exact ligand arrangement around the nanoparticles should be known. Due to the polydispersity, single crystals cannot be grown, unlike in the atomically precise Au-nanoparticles.[29] Still, we expect that, similarly, in the present case there exists a nonspherical arrangement of the ligands, leading to sheets that close towards shells. We trapped the intermediates of self-assembly by rapid cooling of reaction mixture in liquid nitrogen, which shows individual nanoparticles and partially assembled sheet-like structures (Figure S16). Further, the reaction was monitored at different time intervals using TEM which revealed the intermediate structures (Figure S17). The high resolution electron tomography, X-ray powder diffraction patterns, thermoanalytical studies and HR-TEM of capsids further supports the lack of packing order with overall amorphous nature of capsids (Figures S18, S19).

Next, higher level structures based on capsids are pursued by directed self-assembly. We showed above that the carboxylic acid mediated hydrogen bonds stabilize the capsids. Moreover, Figure 2b showed that inter-capsid hydrogen bonding can be achieved but without directionality. It is well known that magnetic forces induce the formation of pearl/necklace-like 1D chains of magnetic nanoparticles.[10] The Co-*p*ABA capsids are superparamagnetic due to their small size of constituent nanoparticles (experimentally determined magnetic core diameter ~3.2 nm, Figure 4a, see Supporting Information for details).[30] First, even application of a very high magnetic field of 9.4 T did not lead to disassembly of the capsids. Instead, directed self-assembly of capsids to 1D chains by induced dipoles of the capsids was observed even using low external magnetic field at 0.65T (Figure 4b). A subtlety is involved, as after removing the magnetic field, the 1D chain of spherical capsids remained intact,

due to inter-capsid hydrogen bondings facilitated by an ensemble of Co-*p*ABA nanoparticles at the two dipoles, as can be shown using TEM, SEM, AFM, and ET reconstruction at zero magnetic field (Figure 4c, Movies S6, S7 and Figures S20-22). The role of the stabilizing hydrogen bonds between the capsids can be further revealed by solvent exchanges. Even if the chains are robust in solvents, which do not disturb the hydrogen bonds (like 1,2-DCB), exposing the capsid chains to acetone leads to slow dis-assembly of the chains with time, due to the gradual opening of the intercapsid hydrogen bonds (Figure 4d). Note that previously the chains of individual nanoparticles have been stable only in the presence of magnetic field and they collapse upon removal of the magnetic field.[11] Our approach can be understood by magnetic field assisted manipulation of the colloidal objects into 1D colloidal chains to drive hydrogen bonding gluing to stabilize the capsid chains.

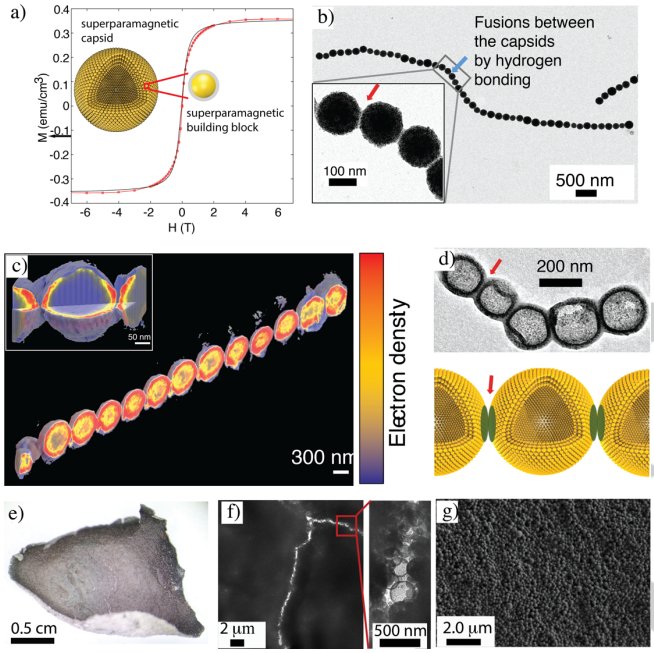

Figure 4. Higher order capsid structures by directed self-assembly. a) Magnetization curve of Co-*p*ABA capsids showing superparamagnetism. b) Supracolloidal 1D chain of 47 capsids. c) ET reconstruction of a capsid chain. d) Capsid chain upon solvent exchange to acetone. The capsid chains are formed by exposing to magnetic field, and after the field removal the chains are stabilized by hydrogen bonds. e) A freestanding film cast from Co-*p*ABA capsids by interfacial self-assembly. f) The dried Co-*p*ABA capsids do not collapse, as revealed using TEM on a fractured surface, allowing to resolve an individual capsid. g) SEM micrograph of the dried film surface showing the packed Co-*p*ABA capsids.

Finally, we extend the processing-directed supramolecular gluing between the capsids towards 3D bulk porous metallic nanoparticle network materials. We used interfacial self-assembly by placing a dispersion of Co-*p*ABA capsids in toluene (15 mg/mL) over a petri-dish containing water. The evaporation of the solvent at the air-water interface leads to self-assembled films (Figure 4e-g, Figure S23). The Co-*p*ABA capsids fuse to bulk self-standing material, as stabilized by the *p*ABA-mediated hydrogen bonds. The capsids do not collapse during drying, as shown in Figure 4f where a fracture surface allows to resolve an individual capsid. Using the Co-*p*ABA with 1.0:0.40 mol ratio, the density of the film is 1.90 g/cm^3, which is 20% of the bulk cobalt matter, where the wall thickness of the porous framework (i.e. capsid) being ca. 25 - 30 nm.

We foresee that synthetic capsid-like colloidally self-assembled materials based on nanoparticles as driven by ligand-driven hydrogen bonds pave ways towards modular functional hollow assembies relevant to reversible confinement and encapsulation.

Acknowledgements

Funding from Academy of Finland for academy professorship (O.I. and H. H), Centre of Excellence in Molecular Engineering of Biosynthetic Hybrid Materials (HYBER, 2014-2019), and ERC Advanced Grant MIMEFUN (2012-2017) are acknowledged. J.V.I.T was supported by the European Commission through the Seventh Framework Programme (FP7) project DynaSLIPS (project number 626954). This work made use of the CSC-IT centre (Espoo) computational facilities and Aalto University Nanomicroscopy Center (Aalto-NMC) premises.

Keywords: colloidal self-assembly • capsids • magnetic nanoparticles • hydrogen bonding • electron tomography

[1] F. Li, D. P. Josephson, A. Stein, *Angew. Chem. Int. Ed.* **2011**, *50*, 360–388.
[2] a) V. N. Manoharan, *Science*, **2015**, *349*, 942; b) M. N. O' Briena, M. R. Jones, C. A. Mirkin, *Proc. Nat. Acad. Sci.* **2016**, *113*, 11717-11725.
[3] a) C. A. Mirkin, R. L. Letsinger, R. C. Mucic, J. J. Storhoff, *Nature*. ***1996***, *382*, 607-609; b) A. P. Alivisatos, K. P. Johnsson, X. Peng, T. E. Wilson, C. J. Loweth, M. P. Bruchez Jr, P. G. Schultz, *Nature* **1996**, *382*, 609–611.
[4] A. K. Boal, F. Ilhan, J. E. DeRouchey, T. Thurn-Albrecht, T. P. Russell, V. M. Rotello, *Nature* **2000**, *404*, 746-748.
[5] L. Manna, D. J. Milliron, A. Meisel, E. C. Scher, A. P. Alivisatos, *Nature Mater.* **2003**, *2*, 382–385.
[6] S. Deka, S. Miszta, D. Dorfs, A. Genovese, G. Bertoni, L. Manna. *Nano Lett.* **2010**,*10*, 3770–3776.
[7] K. Liu, N. N. Zhao, E. Kumacheva, *Chem. Soc. Rev.* **2011**, *40*, 656–671.
[8] a) T. Liu, E. Diemann, H. Li, A. W. Dress, A. Müller, *Nature*, **2003**, *426*, 59-62; b) Y. Xia, T. D. Nguyen, M. Yang, B. Lee, A. Santos, P. Podsiadlo, Z. Tang, S.C. Glotzer, N. A. Kotov, *Nature Nanotechnol.* **2011**, *6*, 580–587;
[9] a) M. M. Maye, I. S. Lim, J. Luo, Z. Rab, D. Rabinovich, T. Liu, C. –J. Zhong, *J. Am. Chem. Soc.* **2005**, *127*, 1519-1529; b) Y. Wang, O. Zeiri, M. Raula, B. L. Ouay, F. Stellacci, I. A. Weinstock, *Nature Nanotechnol.* **2016**, doi:10.1038/nnano.2016.233;
[10] a) J.J. Benkoski, S. E. Bowles, B. D. Korth, R. L. Jones, J. F. Douglas, A, Karim, J. Pyun, *J. Am. Chem. Soc.* **2007**, *129*, 6291–6297; b) J. Pyun, *Angew. Chem. Int. Ed.* **2012**, *51*, 12408-12409.
[11] Z. L. Zhang, Z. Y. Tang, N. A. Kotov, S. C. Glotzer, *Nano Lett.* **2007**, *7*, 1670.
[12] a) C. R. van den Brom, P. Rudolf, T. T. M. Palstra, B. Hessen, *Chem. Commun.* **2007**, 4922; b) C. R. van den Brom, I. Arfaoui, T. Cren, B. Hessen, T. T. M. Palstra, J. T. M. D. Hosson, P. Rudolf, *Adv. Funct. Mater.* **2007**, *17*, 2045–2052.
[13] F. Li, W. C. Yoo, M. B. Beernink, A. Stein, *J. Am. Chem. Soc.* **2009**, *131*, 18548–18555.
[14] M. A. Kostiainen, P. Hiekkataipale, A. Laiho, V. Lemieux, J. Seitsonen, J. Ruokolainen, P. Ceci, *Nat. Nanotechnol.* **2013**, *8*, 52–56.
[15] a) A. H. Gröschel, A. Walther, T. I. Löbling, F. H. Schacher, H. Schmalz, A. H. E. Müller, *Nature* **2013**, *503*, 247–251; b) T. I. Löbling, O. Borisov, J. S. Haataja, O. Ikkala, A. H. Gröschel, A. H. E. Müller. *Nat. Commun.* **2016**, 7,12097.
[16] G. Singh, H. Chan, A. Baskin, E. Gelman, N. Repnin, P. Král, R. Klajn, *Science* **2014**, *345*, 1149-1153.
[17] B. Yoon, W. D. Luedtke, R. N. Barnett, J. Gao, A. Desireddy, B. E. Conn, T. Bigioni, U. Landman, *Nature Mater.* **2014**, *13*, 807–811.

[18] E. Auyeung, T. I. N. G. Li, A.J. Senesi, A. L. Schmucker, B. C. Pals, M. O. de la Cruz, C. A. Mirkin, *Nature*, **2014**, *505*, 73-77.

[19] a) J. Majoinen, J. Hassinen, J. S. Haataja, H. T. Rekola, E. Kontturi, M. A. Kostiainen, R. H. A. Ras, P. Törmä, O. Ikkala, *Adv. Mater.* **2016**, *28*, 5262-5267; b) J.–M. Malho, M. Morits, T. I. Löbling, Nonappa, J. Majoinen, F. H. Schacher, O. Ikkala, A. H. Gröschel, *ACS Macro. Lett.* **2016**, *5*, 1185-1190; c) T. T. T. Myllymäki, Nonappa, H. Yang, V. Liljeström, M. A. Kostiainen, J.-M. Malho, X. X. Zhu, Olli Ikkala, *Soft Matter* **2016**, *12*, 7159-7165.

[20] Nonappa, T. Lahtinen, J. S. Haataja, T.–R. Tero, H. Häkkinen, O. Ikkala, *Angew. Chem. Int. Ed.* **2016,** *55*, 16035-16038.

[21]a) D. J. Kushner, *Bacteriol. Rev*. **1966**, *32*, 302-345; b) S. Katen, A. Zlotnick, *Methods Enzymol*. **2009**, *455*, 395-417; c) A. J. Olson, Y. H. E. Hu, E. Keinan. *Proc. Natl. Acad. Sci.* **2007**, *104*, 20731-20736.

[22] a) F. Caruso, R. A. Caruso, H. Möhwald, *Science*, **1998**, *282*, 1111-1114; b) J. Guo, B. L. Tardy, A. J. Christofferson, Y. Dai, J. J. Richardson, W. Zhu, M. Hu, Y. Ju, J. Gui, R. R. Dagastine, I. Yarovsky, F. Caruso, *Nature Nanotechnol.* **2016**, doi:10.1038/nnano.2016.172; c) H. Kim, E. Pippel, U. Gösele, M. Knez, *Langmuir* **2009**, *25*, 13284-13289; d) Y. Xia, Z. Tang, *Adv. Funct*. Mater. **2012**, *22*, 2585-2593.

[23] M. Yang, H. Chan, G. Zhao, J. H. Bahng, P. Zhang, P. Král, N. A. Kotov, *Nature Chemistry* **2017**, *9*, 287-294.

[24] a) V. F. Puntes, K. M. Krishnan, A. P. Alivisatos, *Science* **2001**, *291*, 2115-2117; b) J. V. I. Timonen, E. T. Seppälä, O. Ikkala, R. A. Ras, *Angew. Chem. Int. Ed.* **2011**, *50*, 2080, 2084.

[25] A. D. Dinsmore, M. F. Hsu, M. G. Nikolaides, M. Marquez, A. R. Bausch, D. A. Weitz, *Science,* **2002**, *298*, 1006-1009.

[26] H. H. Pham, C. D. Taylor, N. J. Henson, *J. Phys. Chem. B*. **2013**, *117*, 868-876.

[27] a) L. Guan, L. Rizzello, G. Battaglia, *Nanomedicine* **2015**, *10*, 2757-2780; b) V. Percec et al, *Science* **2010**, *328*, 1009-1014; c) M. T. Lombardo, L. D. Pozzo, *Langmuir* **2015***, 31*, 1344−1352; d) T. Bian, L. Shang, H. Yu, M. T. Perez, L.-Z. Wu, C.-H. Tung, Z. Nie, Z. Tang, T. Zhang, *Adv. Mater.* **2014***, 26*, 5613–5618.

[28] a) J. Mortensen, L. Hansen, K. Jacobsen, *Phys. Rev. B,* **2005**, *71*, 035109; b) J. Enkovaara, *et. al, J. Phys-Cond. Mat.* **2010***, 22*, 253202.

[29] P.D. Jadzinsky, G. Calero, C.J. Ackerson, D.A. Bushnell, R.D. Kornberg, *Science* **2007**, *318*, 430-433.

[30] J. van Rijssel, B. W. M. Kuipers, B. H. Erne, *J. Magn. Magn. Mater.* **2014**, *353*, 110-115.

Entry for the Table of Contents

COMMUNICATION

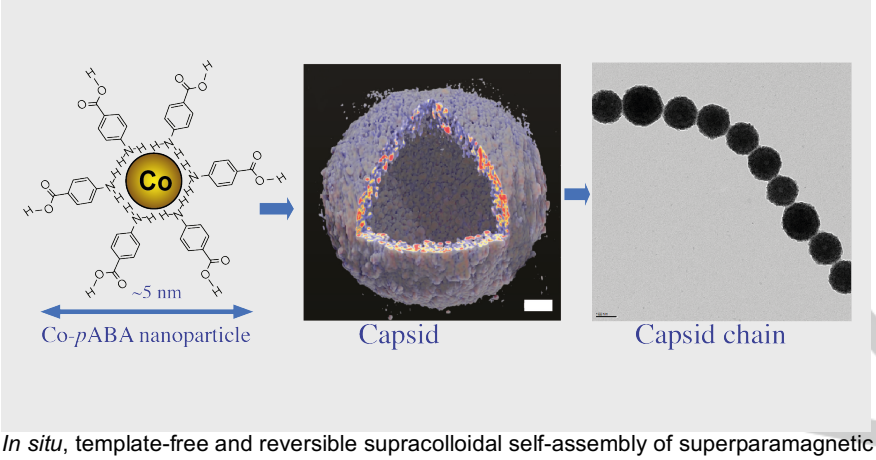

Nonappa, J. S. Haataja, J. V. I. Timonen, S. Malola, P. Engelhardt, N. Houbenov, M. Lahtinen, H. Häkkinen*, O. Ikkala**

Page No. – Page No.

Reversible supracolloidal self-assembly of cobalt nanoparticles to hollow capsids and their superstructures

In situ, template-free and reversible supracolloidal self-assembly of superparamagnetic cobalt nanoparticles to hollow spherical capsids and their directed assembly to higher order superstructures is reported.